

## **Precursor polymorph determines the organic semiconductor structure formed upon annealing.**

Lorenzo Pandolfi<sup>a</sup>, Andrea Giunchi<sup>a</sup>, Arianna Rivalta<sup>a</sup>, Simone D'Agostino<sup>b</sup>, Raffaele Guido Della Valle<sup>a</sup>, Marta Mas-Torrent<sup>c</sup>, Massimiliano Lanzì<sup>a</sup>, Elisabetta Venuti<sup>a,\*</sup>, Tommaso Salzillo<sup>c,d,\*</sup>

<sup>a</sup>Dipartimento di Chimica Industriale "Toso Montanari", University of Bologna, Viale del Risorgimento 4, 40136, Bologna, Italy

<sup>b</sup>Dipartimento di Chimica "G. Ciamician", University of Bologna, Via F. Selmi 2, 40126, Bologna, Italy

<sup>c</sup>Institut de Ciència de Materials de Barcelona, ICMA-B-CSIC, Campus de la UAB, 08193, Bellaterra, Spain

<sup>d</sup>Department of Chemical and Biological Physics, Weizmann Institute of Science, Rehovot 76100, Israel

## **Supporting information**

### Synthesis of N,N-Bis(tert-butyloxycarbonyl)-quinacridone (<sup>t</sup>Boc-QA)

Quinacridone (QA, 1.15 g, 3.68 mmol), di-tert-butyl dicarbonate (<sup>t</sup>Boc<sub>2</sub>O) (3.87 g, 17.7 mmol), 4-dimethylaminopyridine (DMAP) (0.90 g, 7.37 mmol) were mixed in CH<sub>2</sub>Cl<sub>2</sub> (184 mL) and reacted under an inert atmosphere for 48 h at room temperature. The solvent was then removed at reduced pressure and the crude product was purified by column chromatography (SiO<sub>2</sub>, toluene/ethyl acetate 9:1). The resulting product was recrystallized several times from ethyl acetate to give 0.96 g (1.87 mmol) of a yellow solid (51% yield).

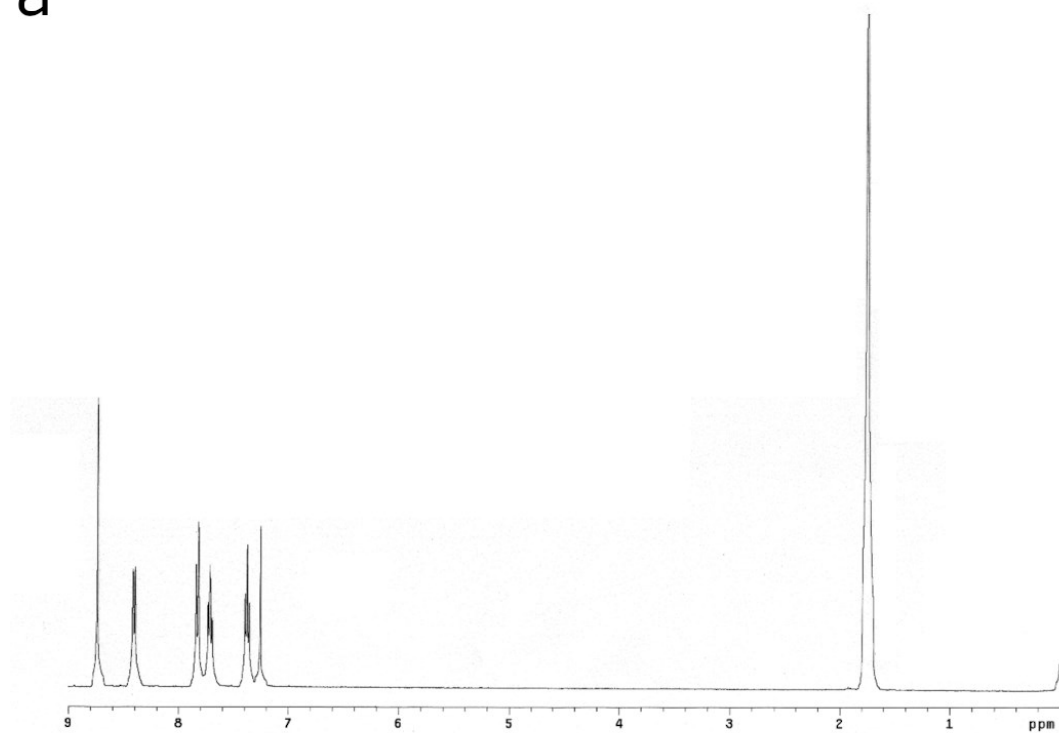
### NMR and Mass spectroscopy

<sup>1</sup>H NMR spectra were recorded on a Varian Mercury Plus (400 MHz) spectrometer using tetramethylsilane as a reference. Mass spectroscopy (electrospray ionization, ESI) spectra were carried out on a Waters XEVO Q-TOF instrument.

<sup>1</sup>H NMR (400 MHz, CDCl<sub>3</sub>) δ 8.74 (s, 2H, H<sub>A</sub>), 8.41 (dd, J = 8.01, 1.56 Hz, 2H, H<sub>B</sub>), 7.84 (d, J = 8.79 Hz, 2H, H<sub>C</sub>), 7.72 (m, J = 8.49, 7.13, 1.56 Hz, 2H, H<sub>D</sub>), 7.38 (t, 7.52 Hz, 2H, H<sub>E</sub>), 1.77 (s, 18H, -CH<sub>3</sub>).

MS: m/z 513 [M]<sup>+</sup>; 457 [M-C<sub>4</sub>H<sub>8</sub>]<sup>+</sup>; 413 [M-C<sub>5</sub>H<sub>8</sub>O<sub>2</sub>]<sup>+</sup>; 357 [M-2(C<sub>4</sub>H<sub>8</sub>)]<sup>+</sup>; 313 [M-2(C<sub>5</sub>H<sub>8</sub>O<sub>2</sub>)]<sup>+</sup>.

a



b

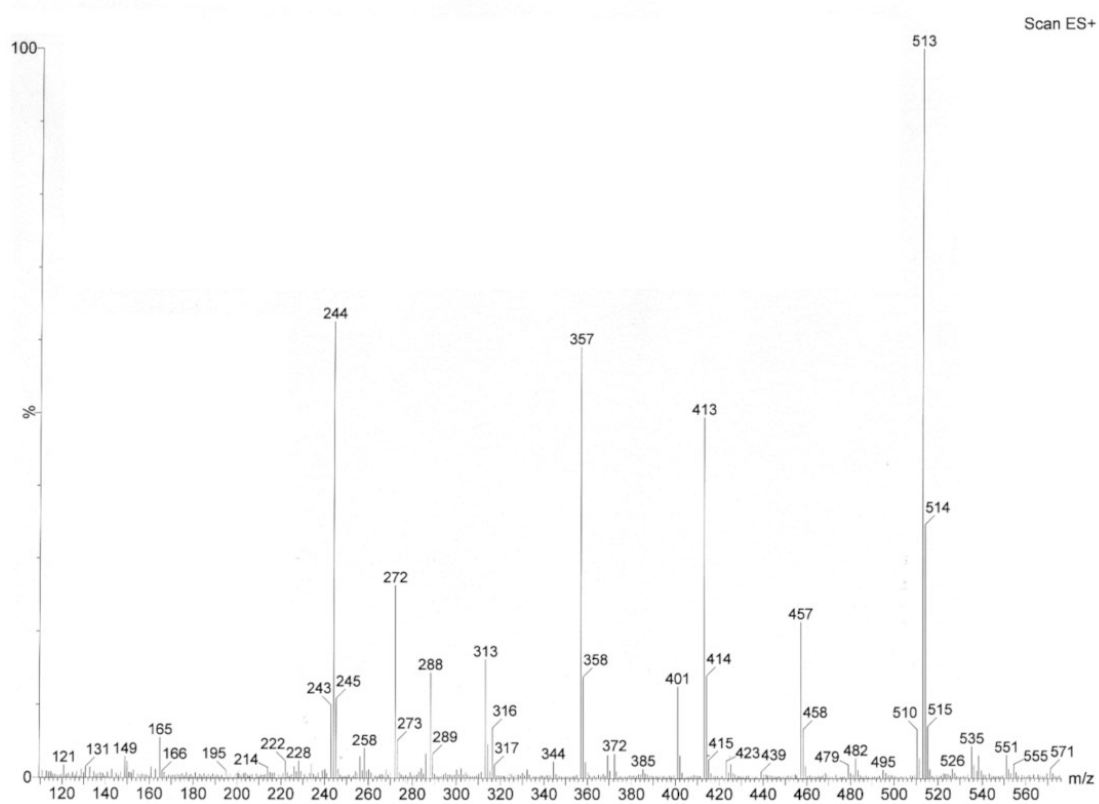


Figure S 1 Upper panel: <sup>1</sup>H NMR spectrum of *t*-Boc-QA in CDCl<sub>3</sub> (the singlet at 7.24 ppm is ascribable to CHCl<sub>3</sub>). Lower panel: mass spectrum (positive ions) of *t*-Boc-QA.

## X-ray single crystal structures of <sup>t</sup>Boc-QA polymorphs I and II.

**Table S1.** Crystal data and refinement details for crystalline <sup>t</sup>Boc-QA form I and form II.

	<b>Form I</b>	<b>Form II</b>
<b>Formula</b>	C <sub>30</sub> H <sub>28</sub> O <sub>6</sub> N <sub>2</sub>	C <sub>30</sub> H <sub>28</sub> O <sub>6</sub> N <sub>2</sub>
<b>fw</b>	512.54	512.54
<b>Temperature (K)</b>	RT	RT
<b>Cryst. System</b>	Monoclinic	Monoclinic
<b>Space group</b>	P2 <sub>1</sub> /n	P2 <sub>1</sub> /c
<b>Z</b>	2	4
<b>a (Å)</b>	14.1499(10)	23.791(3)
<b>b (Å)</b>	6.5255(6)	6.1680(10)
<b>c (Å)</b>	14.3577(11)	19.031(3)
<b>α (deg)</b>	90	90
<b>β (deg)</b>	105.550(8)	112.076(18)
<b>γ (deg)</b>	90	90
<b>V (Å<sup>3</sup>)</b>	1277.20(18)	2587.9(8)
<b>D<sub>calc</sub> (g/cm<sup>3</sup>)</b>	1.333	1.316
<b>μ (mm<sup>-1</sup>)</b>	0.093	0.092
<b>Measd reflns</b>	4659	18121
<b>Indep reflns</b>	2244	5974
<b>Largest diff. peak/hole (e/Å<sup>3</sup>)</b>	0.14/-0.14	0.16/-0.16
<b>R<sub>1</sub>[on F<sub>o</sub><sup>2</sup>, I&gt;2σ(I)]</b>	0.0476	0.0583
<b>wR<sub>2</sub> (all data)</b>	0.1124	0.1050

At ambient conditions, the latent pigment <sup>t</sup>Boc-QA may appear in two different polymorphic modifications, named here form I and II. The former corresponds to the already known crystal structure of this compound,<sup>1</sup> and can be prepared by conventional recrystallization from ethyl acetate of the as-synthesized material. The latter was identified in this work by lattice phonon Raman microscopy and XRD on specimens obtained by drop-casting acetone solutions onto glass at 75°C and in films prepared by the BAMS method (see main text).

<sup>t</sup>Boc-QA form I structure was redetermined in this work by single-crystal X-ray analysis. The crystal is monoclinic with space group P2<sub>1</sub>/n and cell parameters a = 14.149(1)Å, b = 6.5255(6)Å, c = 14.357(1)Å, β = 105.550(8)°. There are two centrosymmetric molecules per cell, with the

asymmetric unit consisting of half a molecule. The tert-butoxycarbonyl group bonded to the N-atom is twisted by  $54.3(2)^\circ$  from the heterocyclic ring to which it is attached and the condensed ring system is not perfectly planar, as the dihedral angle between two condensed rings is found to be  $\approx 175^\circ$ . No specific intermolecular interactions are present. Translationally equivalent molecules of  ${}^t\text{Boc-QA}$  are arranged with the aromatic rings forming stacks in a face-to-face fashion.

The crystal structure of  ${}^t\text{Boc-QA}$  form II was also determined by single-crystal X-ray analysis. The unit cell is monoclinic with space group  $P2_1/c$  and cell parameters  $a = 23.791(3) \text{ \AA}$ ,  $b = 6.1680(10) \text{ \AA}$ ,  $c = 19.031 \text{ \AA}$ ,  $\beta = 112.076(18)^\circ$ . There are four centrosymmetric molecules per cell, with the asymmetric unit consisting of two half molecules, denoted as A and B. Each  ${}^t\text{Boc}$  group is twisted with respect to the corresponding heterocyclic ring by  $64.5(5)^\circ$  and  $77.6(5)^\circ$  for molecules A and B, respectively. The condensed ring systems are, again, not perfectly planar, with a dihedral angle between the central benzene ring and the neighboring ones of  $\approx 175^\circ$  and  $177^\circ$  for molecules A and B, respectively. Form II structure features two distinct sets of face-to-face stacks generated by the translation of the independent A and B molecules.

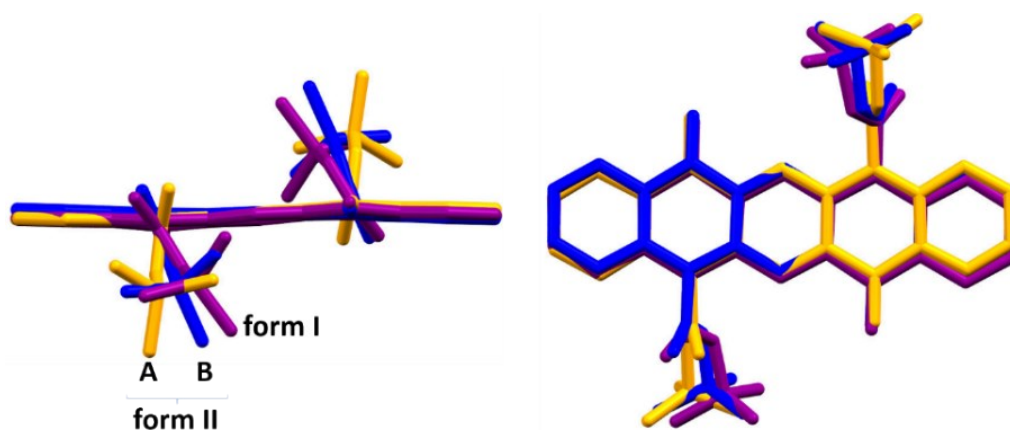


Figure S 2 Side and top views of the overlap among the molecules of  ${}^t\text{Boc-QA}$  present in forms I and II showing the main differences in the orientation of the  ${}^t\text{Boc}$  group with respect to the aromatic system. Form I in purple, form II in blue and orange for molecules A and B, respectively.  $H_{\text{CH}}$  atoms omitted for clarity.

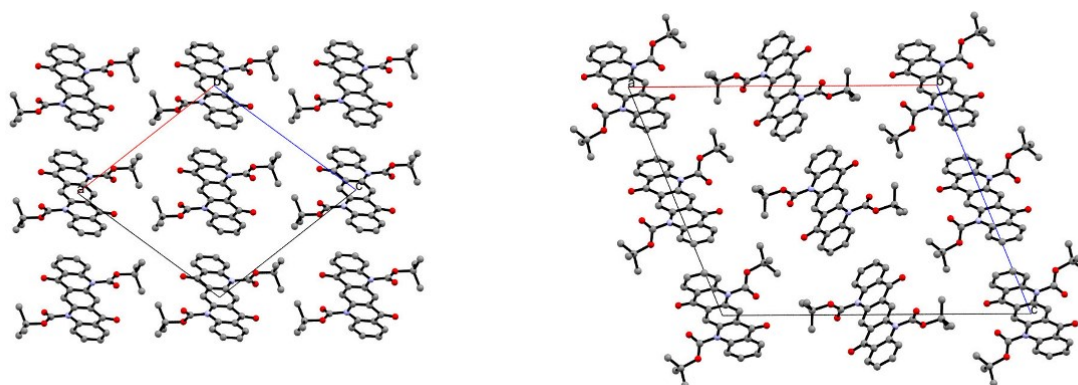


Figure S 3 Crystal packing diagrams viewed along the  $b$ -axis for  ${}^t\text{Boc-QA}$  form I (left) and form II (right).  $H_{\text{CH}}$  atoms omitted for clarity.

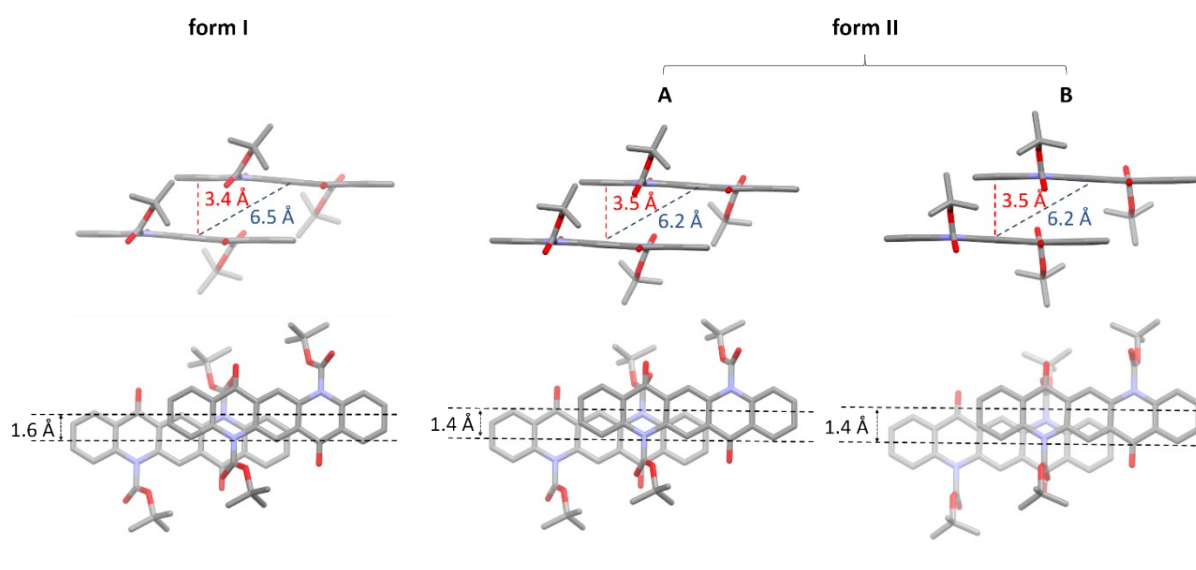


Figure S 4 Comparison of the face-to-face stacking arrangements detected within crystalline <sup>t</sup>Boc-QA form I and II. H<sub>CH</sub> atoms omitted for clarity.

### Thermochemical cleavage of the <sup>t</sup>Boc protection group

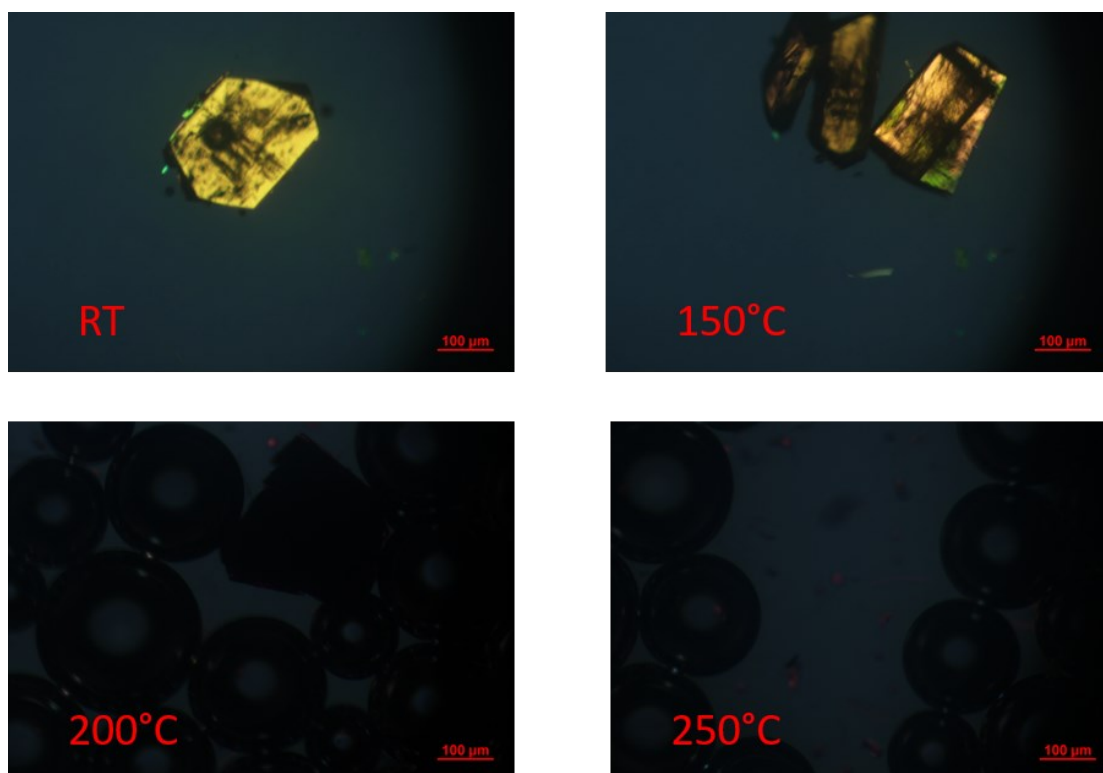


Figure S 5 Optical photographs under polarized light of a crystal of <sup>t</sup>Boc-QA form I taken during the thermal deprotection process.

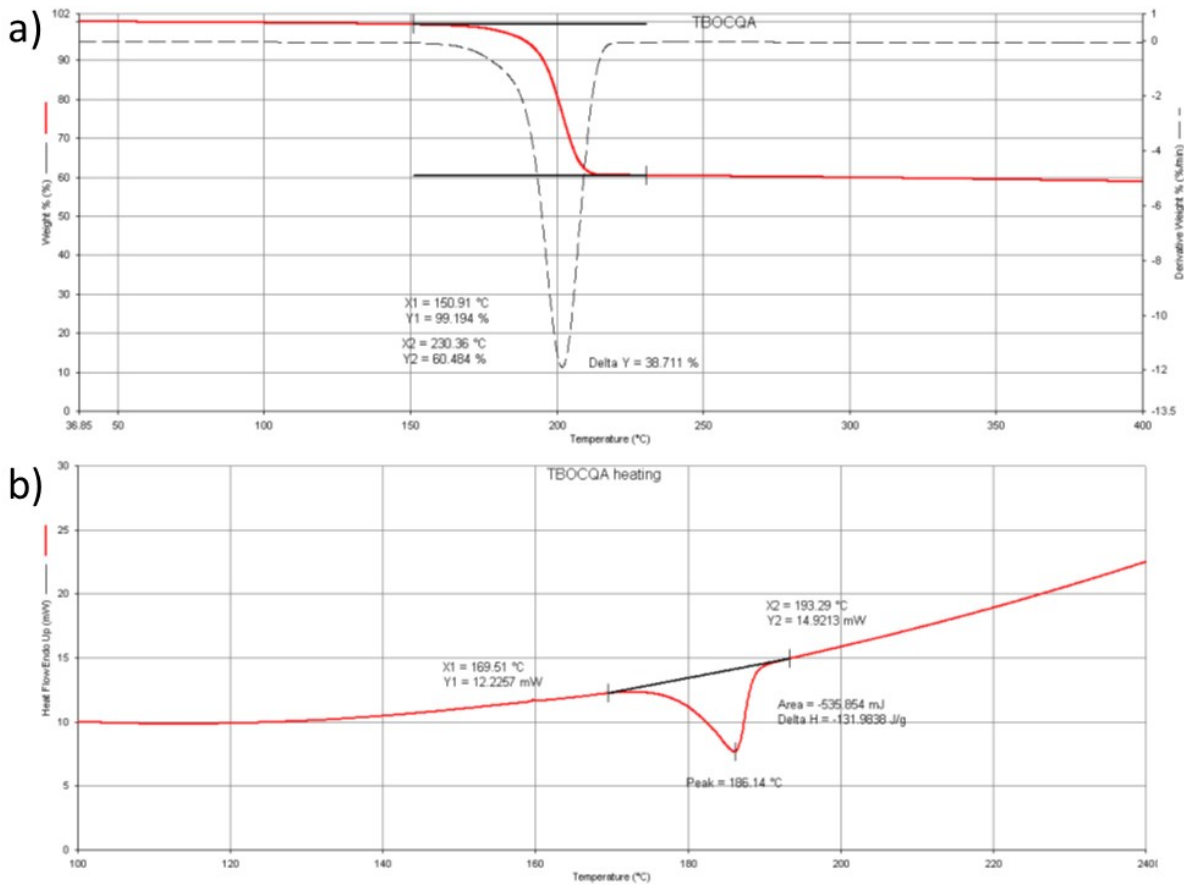


Figure S 6 a) Thermogram of a polycrystalline sample of <sup>1</sup>Boc-QA form I; DSC trace of a polycrystalline sample of <sup>1</sup>Boc-QA form I.

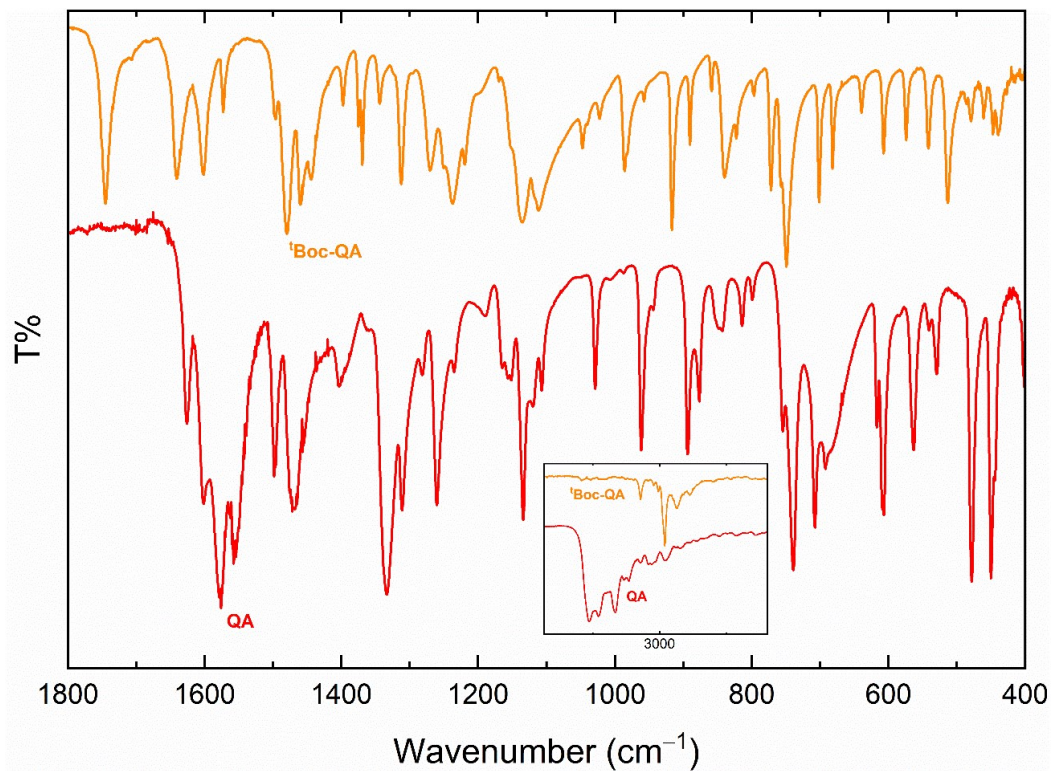


Figure S 7 IR spectra of <sup>1</sup>Boc-QA before (orange trace) and after (red trace) the thermochemical cleavage of the <sup>1</sup>Boc protection groups. In the inset the details of the N-H stretching region used to assess the reaction progression.



## Raman characterization of <sup>1</sup>Boc-QA polymorphs

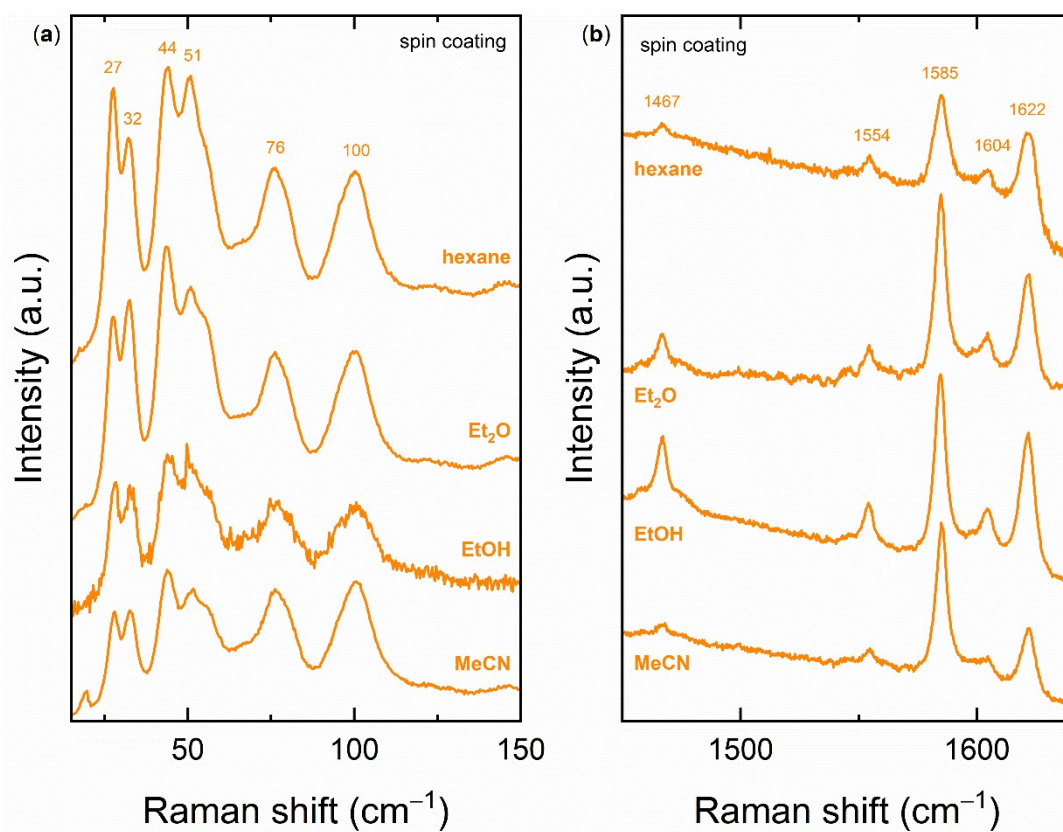


Figure S 8 Raman Spectra in the lattice phonon range (left) and in the 1400-1700 cm<sup>-1</sup> intramolecular range (right) for <sup>1</sup>Boc-QA films obtained by the spin coating technique with solution of various solvents. In all cases the presence of the <sup>1</sup>Boc-QA crystal form I is confirmed by the lattice phonon pattern.

Figure S9 shows the Raman spectra in the lattice phonon region for the crystallite obtained by drop casting <sup>1</sup>Boc-QA acetone solutions on a glass substrate at RT (left) and at 75°C (right). The two coloured traces correspond to the spectra of randomly oriented crystallites. The differences between the spectral features of the patterns allow for the identification of the two different crystal forms I and II. Such an identification is also supported by the Raman analysis in polarized light. Spectra identified in the Figure with the PARPAR, PERPER and PARPER labels correspond to polarized light measurements performed in backscattering geometry on single crystals oriented along their extinction directions, as shown by the arrows in the Figure. For monoclinic systems like those under study, such a direction is either parallel/perpendicular to the *b* crystal axis or lies in the *ac* crystal plane, and such a knowledge is used to align the crystal axes with respect to the laboratory reference frame. In both the measurement configurations labelled PARPAR and PERPER in the Figure, the spectra are collected keeping incident and scattered light linearly polarized parallel to each other,



while the crystal has been rotated by 90°. In the spectra labelled as PARPER incident and scattered light are crossed polarized.

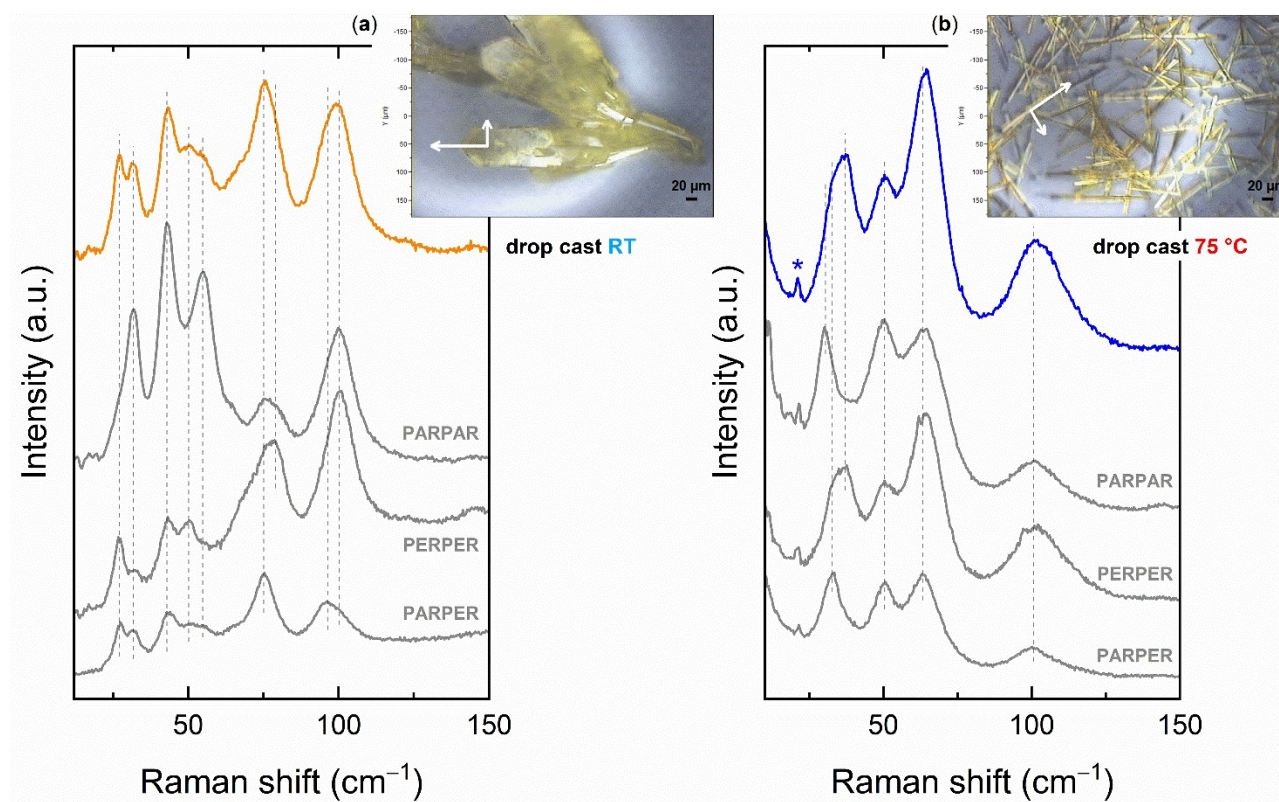


Figure S 9 Raman spectra in the lattice phonon region of <sup>14</sup>Boc-QA crystallites obtained from the drop cast of acetone solutions at RT (left) and at 75°C (right) on a glass substrate. The optical images show the two different observed morphologies, and the arrows indicate the crystal extinction directions as detected in that area of the sample. The RT deposition is found to yield <sup>14</sup>Boc-QA form I; the 75°C yields form II. The asterisk marks a band of the substrate.

Following the symmetry Raman selection rules, and in agreement with symmetry properties of the polarizability tensor which governs the intensity of the Raman signal, the polarized light Raman measurements allow for the selective detection of vibrational modes of different symmetry. In this work, in which they are used to discriminate more effectively between two crystalline forms, the change in the relative peak intensities of the various measurement geometries allows for a better definition of the spectral features both in the single crystals and in the films.

The red and black traces of Figure S10 correspond to the two typical Raman patterns detected in the lattice phonon region when <sup>14</sup>Boc-QA films fabricated by the BAMS method are kept at a fixed orientation with respect to the laboratory reference frame and are measured in parallel polarized light, as explained in the main text of this work. In the Figure the spectra are compared to the polarized Raman spectra collected on a single crystal.

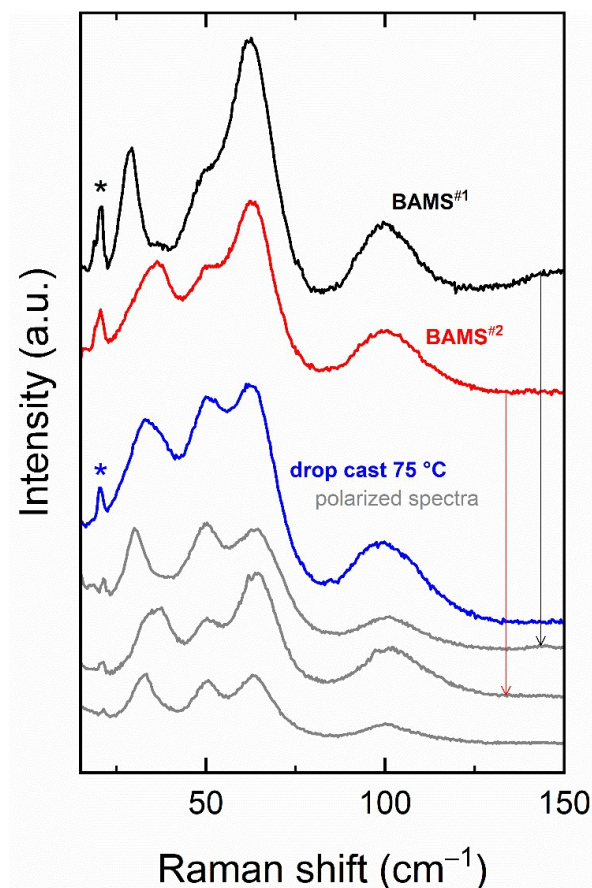


Figure S 10 The two typical form II lattice phonon Raman patterns observed in the <sup>t</sup>Boc-QA films prepared by BAMS method compared to the polarized light spectra of form II single crystal (see also Figure S 9). The asterisk marks a band of the substrate.

### DFT Calculations of QA and <sup>t</sup>Boc-QA normal vibrational modes

To aid the normal mode assignments for the bands detected in the vibrational spectra of QA and <sup>t</sup>Boc-QA DFT simulations were performed. All calculations used GAUSSIAN 16 program package<sup>2</sup>. The geometry optimization and energy calculations were carried out using B3LYP/6-311G++\*\* functional/basis-set and the frequencies computed at the harmonic level were scaled by the factor given for this combination<sup>3</sup>. For the frequency range used as diagnostic for the thermal deprotection, a comparison between simulated and experimental spectra is shown in Figure S10. Tables S2,S3 report the calculated frequencies and the representations of the eigenvectors for the selected modes of the two species. The isolated QA molecule possesses C<sub>2h</sub> symmetry, and the normal modes classify as A<sub>g</sub>, B<sub>g</sub>, A<sub>u</sub> and B<sub>u</sub>. All the in-plane Raman active modes belong to the total symmetric representation A<sub>g</sub>. The inversion centre (with the g/u character) is preserved in all the crystal structures. The isolated <sup>t</sup>Boc-QA belongs to the C<sub>i</sub> symmetry group and normal modes classify as A<sub>g</sub>, A<sub>u</sub>, with those belonging to the total symmetric representation A<sub>g</sub> being Raman active. The

inversion centre is preserved in crystal form I; in crystal form II the molecule lies in a general position but with a geometry only slightly different from the that of isolated molecule.

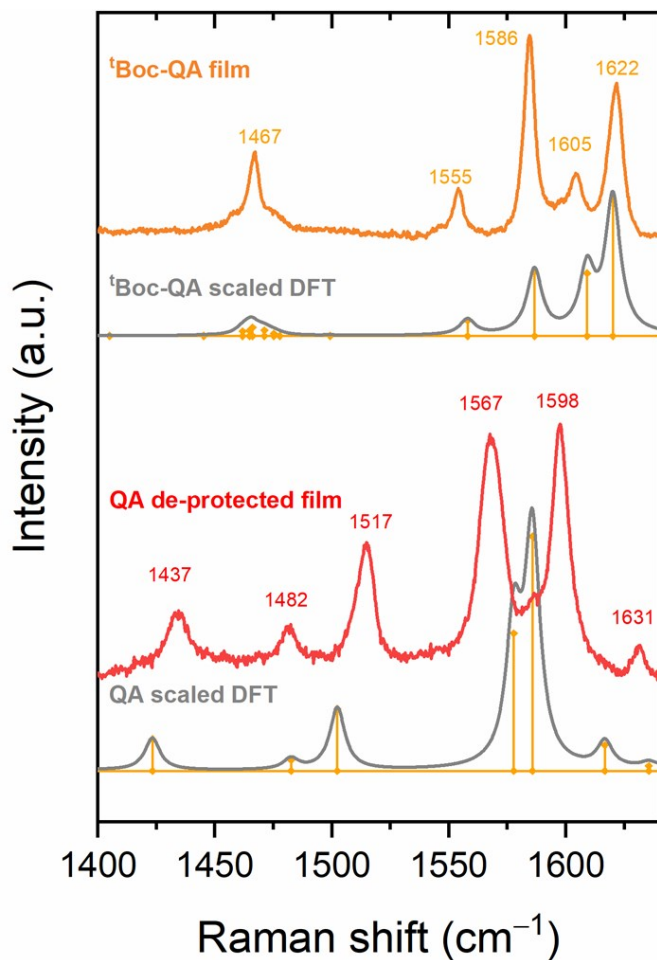


Figure S 11 Experimental and calculated Raman spectra in the energy range of the intramolecular vibrations used to monitor the thermal de-protection of the films.

Table S 2 Experimental and computed wavenumbers for the normal modes of QA in the interval 1400-1600  $\text{cm}^{-1}$ , with symmetry assignments and eigenvector graphical representations.

Exp frequency ( $\text{cm}^{-1}$ )	Symmetry	Scaled DFT frequency ( $\text{cm}^{-1}$ )	Eigenvectors
1437	$A_g$	1423	
1482	$A_g$	1483	
1517	$A_g$	1502	

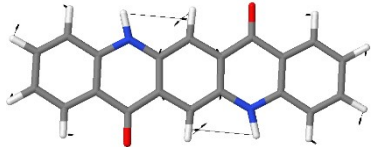


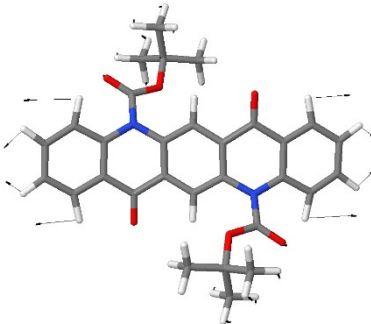
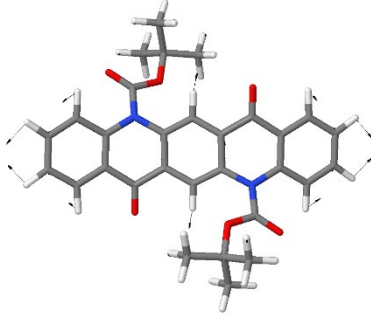
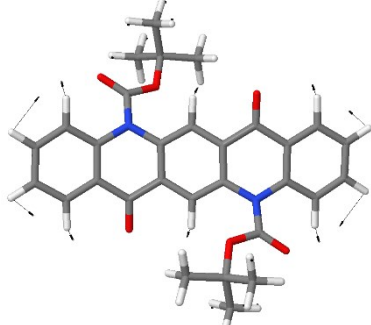
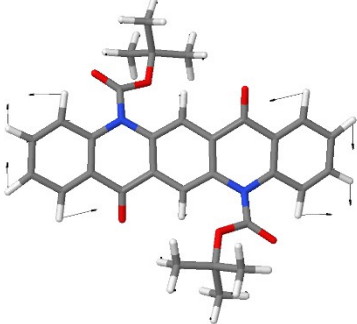
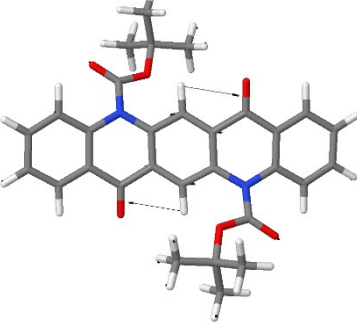
1567	$A_g$	1578	
1598	$A_g$	1586	
1631	$A_g$	1616	

Table S 3 Experimental and computed wavenumbers for the normal modes of  $^1\text{Boc-QA}$  in the interval  $1400\text{-}1600\text{ cm}^{-1}$ , with symmetry assignments and eigenvector graphical representations.

Exp frequency ( $\text{cm}^{-1}$ )	Symmetry	Scaled DFT frequency ( $\text{cm}^{-1}$ )	Eigenvector
1467	$A_g$	1475	
1555	$A_g$	1558	
1586	$A_g$	1587	

1605	$A_g$	1608	
1622	$A_g$	1620	

## References

1. Mizuguchi, J. Di-tert-butyl 7, 14-dihydro-7, 14-dioxo-quinolo[2,3-b]acridine-5, 12-dicarboxylate. *Acta Crystallogr. Sect. E* **59**, o474–o475 (2003).
2. Gaussian 16, Revision A.03, M. J. Frisch, G. W. Trucks, H. B. Schlegel, G. E. Scuseria, M. A. Robb, J. R. Cheeseman, G. Scalmani, V. Barone, G. A. Petersson, H. Nakatsuji, X. Li, M. Caricato, A. V. Marenich, J. Bloino, B. G. Janesko, R. Gomperts, B. Mennucci, H. P. Hratchian, J. V. Ortiz, A. F. Izmaylov, J. L. Sonnenberg, D. Williams-Young, F. Ding, F. Lipparini, F. Egidi, J. Goings, B. Peng, A. Petrone, T. Henderson, D. Ranasinghe, V. G. Zakrzewski, J. Gao, N. Rega, G. Zheng, W. Liang, M. Hada, M. Ehara, K. Toyota, R. Fukuda, J. Hasegawa, M. Ishida, T. Nakajima, Y. Honda, O. Kitao, H. Nakai, T. Vreven, K. Throssell, J. A. Montgomery, Jr., J. E. Peralta, F. Ogliaro, M. J. Bearpark, J. J. Heyd, E. N. Brothers, K. N. Kudin, V. N. Staroverov, T. A. Keith, R. Kobayashi, J. Normand, K. Raghavachari, A. P. Rendell, J. C. Burant, S. S. Iyengar, J. Tomasi, M. Cossi, J. M. Millam, M. Klene, C. Adamo, R. Cammi, J. W. Ochterski, R. L. Martin, K. Morokuma, O. Farkas, J. B. Foresman, and D. J. Fox, Gaussian, Inc., Wallingford CT, (2016.)
3. <https://cccbdb.nist.gov/vsfx.asp>; M. P. Andersson and P. Uvdal; New Scale Factors for Harmonic Vibrational Frequencies Using the B3LYP Density Functional Method with the Triple- $\zeta$  Basis Set 6-311+G(d,p); *J. Phys. Chem. A* 2005, 109, 12, 2937–2941; 10.1021/jp045733a